Quench Performance of a 1 m Long Single-Aperture 11 T Nb_3Sn Dipole Model for LHC Upgrades

A.V. Zlobin, N. Andreev, G. Apollinari, B. Auchmann, H. Bajas, E. Barzi, R. Bossert, G. Chlachidze, M. Karppinen, F. Nobrega, I. Novitski, L. Rossi, D. Smekens, D. Turrioni

***Abstract*— FNAL and CERN are performing a joint R&D program with the goal to build a 5.5-m long twin-aperture 11 T Nb_3Sn dipole prototype suitable for installation in the LHC. An important part of the program is the development and test of a series of short single-aperture and twin-aperture models with a nominal field of 11 T at the LHC nominal current of 11.85 kA and 20% margin. This paper describes design features and test results of a 1 m long single-aperture Nb_3Sn dipole model fabricated and tested at FNAL.**

***Index Terms*— Accelerator magnets, Large Hadron Collider, superconducting coils, magnet test.**

I. Introduction

The planned upgrade of the Large Hadron Collider (LHC) collimation system requires additional collimators to be installed in the dispersion suppressor areas around points 2, 3 and 7, as well as around the high luminosity interaction regions [1]. Replacing some 8.33 T 15 m long NbTi LHC main dipoles (MB) with shorter 11 T Nb_3Sn dipoles compatible with the accelerator lattice and the LHC main systems could provide the required longitudinal space for the collimators. These twin-aperture dipoles operating at 1.9 K and powered in series with the main dipoles should deliver the same integrated strength of 119 Tm at the operational current of 11.85 kA.

To demonstrate feasibility, CERN and FNAL have started a joint R&D program with the goal to develop and build a 5.5 m long twin-aperture Nb_3Sn dipole prototype for the LHC collimation system upgrade. Two such dipoles with a collimator in between will replace one 15 m long MB dipole. The program started at the end of 2010 with the design and construction of a 2 m long single-aperture Nb_3Sn demonstrator magnet (MBHSP01) [2] which was tested at FNAL in June 2012 and reached 10.4 T at the LHC operating temperature of 1.9 K [3]. To improve the magnet quench performance and field quality, as well as to demonstrate performance reproducibility, the fabrication of a series of 1 m long collared coils was started at FNAL last year. These collared coils will be tested first in a single-aperture configuration and then assembled and tested inside a common iron yoke (twin-aperture configuration). In parallel, four 2 m long collared coils will be built and tested at CERN first in a single-aperture and then in a twin-aperture configuration to establish the technology transfer to CERN, and demonstrate and optimize the quench performance, field quality and quench protection of Nb_3Sn coils and a somewhat different mechanical concept of the collar and yoke [4].

This paper describes the design features of the first 1 m long single-aperture Nb_3Sn dipole model (MBHSP02) fabricated at Fermilab and tested in April 2013. Test results presented in this paper include magnet quench performance and protection heater studies at 1.9 K and 4.5 K. The results of magnetic measurements are reported elsewhere [5].

II. Magnet Design and Construction

The design concepts of 11 T Nb_3Sn dipole in single-aperture and twin-aperture configurations are described in [3, 4]. The coil cross-section was optimized to provide a dipole field above 11 T in a 60 mm aperture at the 11.85 kA current with 20% margin, and geometrical field errors below 10^{-4}. The calculated design parameters of the 2 m long single- and twin-aperture dipole magnets are reported in [6]. For a 1 m long model in the single-aperture configuration, the calculated nominal parameters are slightly higher (for example, the central field is 11.07 T at I_{nom}=11.85 kA) due to field enhancement in the magnet center from the coil ends. The cross-sections of the single-aperture cold mass (FNAL design) is shown in Fig. 1.

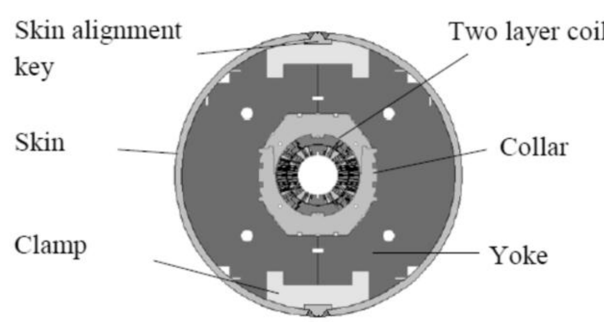

Fig. 1. Cross-section of the 11 T dipole cold mass.

The coils in MBHSP02 were made of 40-strand Rutherford cable with a stainless steel core and a new R&D strand [7]. The 0.025 mm thick and 11 mm wide core is used to reduce interstrand eddy currents in the cable. The 0.7 mm Nb_3Sn RRP-150/169 strand has smaller sub-element size of ~35 µm to reduce the persistent current effect and improve cable stability with respect to the flux jumps. Cross-section of the strand and a picture of the cored cable are shown in Fig. 2.

Manuscript received July 15, 2013. Work supported by Fermi Research Alliance, LLC, under contract No. DE-AC02-07CH11359 with the U.S. Department of Energy and European Commission under FP7 project HiLumi LHC, GA no. 284404.

N. Andreev, G. Apollinari, E. Barzi, R. Bossert, G. Chlachidze, F. Nobrega, I. Novitski, D. Turrioni, A.V. Zlobin are with Fermi National Accelerator Laboratory, P.O. Box 500, Batavia, IL 60510, USA (phone: 630-840-8192; fax: 630-840-8079; e-mail: zlobin@fnal.gov).

B. Auchmann, H. Bajas, M. Karppinen, L. Rossi, D. Smekens are with the European Organization for Nuclear Research, CERN CH-1211, Genève 23, Switzerland.

Fig. 2. RRP-150/169 strand and insulated 40-strand cable with a SS core.

Each coil consists of 2 layers and 56 turns wound from a single ~100 m long piece of cable wraped with 0.075 mm thick and 12.7 mm wide E-glass tape with ~50% overlap. The coil poles were made of Ti alloy, and wedges, end spacers and saddles were made of stainless steel. Based on the MBHSP01 test results and autopsy, the length of the coil end spacers was reduced to minimize the gaps between them and block turns after reaction. The saddles were optimized to avoid coil lead overcompression during coil reaction and magnet assembly.

Coils were made using the wind-&-react method. During winding each coil layer was filled with CTD-1202X liquid ceramic binder and cured under a small pressure at 150ºC for 0.5 hr. During curing the coil inner and outer layers were shimmed in the mid-plane to a size 1.0 and 1.5 mm respectivelly smaller than the nominal coil size to provide room for the Nb_3Sn cable expantion during reaction [8]. Each coil was reacted in Argon using a 3-step cycle with T_{max}=665^{o}C for 50 hrs. Then, the coils were impregnated with CTD101K epoxy and cured at 125°C for 21 hrs.

Two coils (#5 and #7) surrounded by the ground insulation and stainless steel protection shells were clamped by stainless steel collar blocks. These blocks were previously used in MBHSP01. The coil ground insulation consists of 1 layer of 0.114 mm thick Kapton film with adhesive and 4 layers of 0.125 mm thick Kapton film.

Two identical quench protection heaters composed of 0.025 mm thick stainless steel strips were mounted on each side of the coil between the 1st and 2nd Kapton layers of the ground insulation (Fig. 3, left). The heater position inside the ground insulation was chosen based on the results of heater test in MBHSP01dipole demonstrator [9]. The width of strips quenching high field (HF) and low field (LF) blocks are 26 mm and 21.5 mm respectively (Fig. 3, right). The strips on each side of each coil were connected in series forming two identical heater circuits.

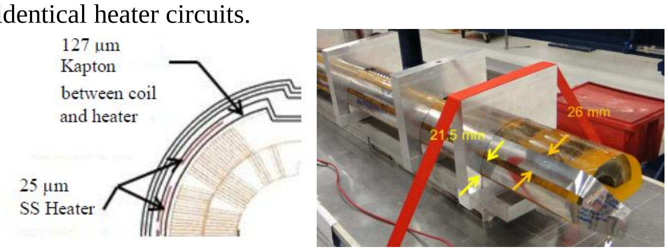

Fig. 3. Ground insulation with protection heaters.

The collared coil was installed inside a vertically split iron yoke with a 400 mm outer diameter and fixed with Al clamps. The yoke length covered the entire coil length including the Nb_3Sn/NbTi lead splices. The 12 mm thick bolted skin made of stainless steel surrounds the yoke and provides the coil final pre-compression. Two 50 mm thick stainless steel end plates bolted to the shell restrict the axial coil motion.

The magnet mechanical structure and the coil pre-stress were optimized to keep the coil stress below 165 MPa during magnet assembly and operation. This prestress maintains the coils under compression up to the ultimate design field of 12 T [4]. The coil prestress was provided by the coil midplane and radial shims installed inside the collared coil as well as the collar-yoke shims placed in the midplane area [10]. The mid-plane and collar-yoke shims were tapered to avoid coil end overcompression. During magnet assembly the prestress was controlled by strain gauges installed on the coil inner surface in two cross-sections along the coil straight section. However, this instrumentation did not provide reliable information on the coil preload after cool-down and during excitations.

III. Test Results

MBHSP02 was tested at FNAL Vertical Magnet Test Facility [11]. The coils were instrumented with voltage taps and a quench antenna to detect and localize quenches during magnet quench performance and protection heater studies. The voltage tap scheme for one of the coils and relative position of pick-up coils of the quench antenna are shown in Fig. 4.

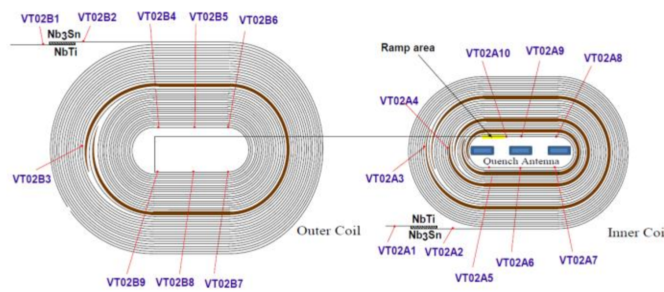

Fig. 4. Voltage tap scheme in the 11 T dipole coil.

The MBHSP02 quench current limits, estimated based on measured witness sample data, are 14.3 kA at 4.5 K and 16 kA at 1.9 K, corresponding to bore fields of 12.7 T and 14.1 T respectively. Note that the maximum design field for this magnet is 12 T, limited by the coil pre-stress level.

A. Quench Performance

The training quenches both at 4.5 K and 1.9 K are shown in Fig. 5. Magnet training started at 4.5 K with a regular current ramp rate of 20 A/s. The first quench at 9.57 kA corresponds to 72% of the short sample limit (SSL) at 4.5 K. After 17 quenches in the inner-layer end blocks of both coils, a few quenches were detected in the outer-layer mid-plane blocks *b2_b3* of coil #7 (circles in Fig. 5).

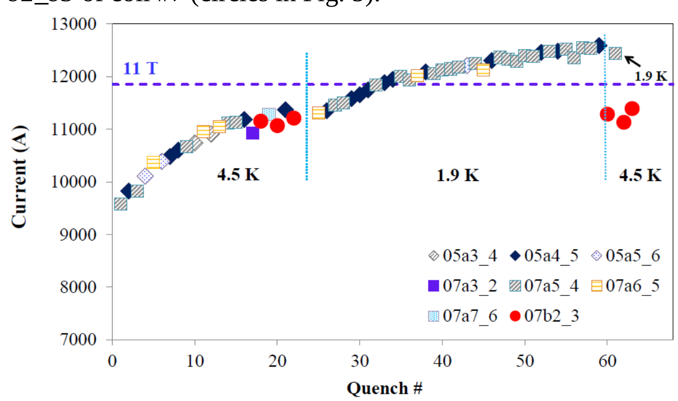

Fig. 5. Magnet training.

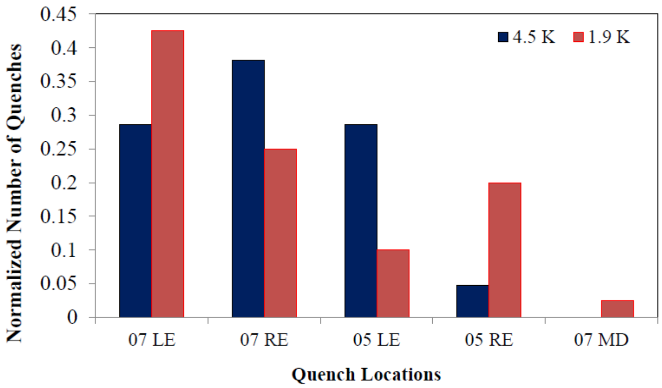

Fig. 6. Quench location during magnet training.

The magnet training was then continued at 1.9 K. The magnet nominal field of 11 T was reached after 30 training quenches. The maximum field in the aperture was 11.7 T or 97.5% of the magnet design field. All quenches at 1.9 K also occurred in the inner-layer blocks *a3_a4* and *a4_a5* of both coils. Quench multiplicity in coils with the longitudinal quench location is shown in Fig. 6. Few quenches at 4.5 K and one quench at 1.9 K after the magnet training at 1.9 K illustrate the magnet training memory (Fig. 5).

In order to check stability of the magnet operation, so called hold-to-quench test was performed both at 4.5 K and 1.9 K. The magnet current was ramped up at 10-20 A/s to a pre-set value and then was held until quench. Fig. 7 shows the holding time to quench vs. current at 4.5 K and 1.9 K. Data with zero holding time represents the regular quenches with the highest current at 20 A/s at the end of magnet training. All the holding quenches except for those with zero holding time started in the outer-layer mid-plane block *b2_b3* of coil #7. The voltage development during holding quenches was non-linear and very reproducibile.

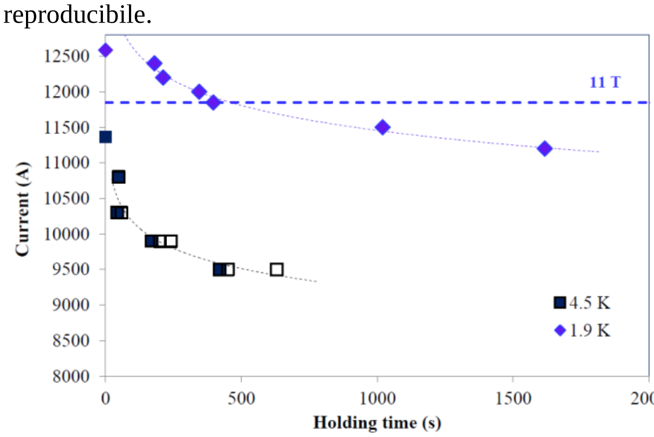

Fig. 7. Holding time to quench vs. plateau current.

Ramp rate dependences of the magnet quench current and quench locations at 4.5 K and 1.9 K are shown in Fig. 8. The stainless steel core used in this model suppressed cable eddy currents and significantly reduced the magnet ramp rate sensitivity at the high current ramp rates. There is a negative ramp rate dependence at ramp rates below 20 A/s at both temperatures. Extrapolation of the quench currents to dI/dt=0 at 4.5 K and 1.9 K gives the I_{max} ~12 kA and ~13.5 kA respectively that is noticeably lower than the magnet SSL.

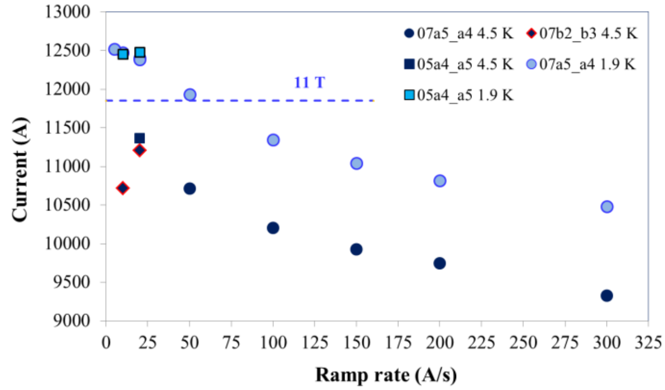

Fig. 8. Ramp rate sensitivity of magnet quench current.

The temperature dependences of the magnet quench current measured at 20 A/s and 50 A/s are shown in Fig. 9. All the quenches at 50 A/s and quenches at intermediate temperatures below 4 K at 20 A/s were initiated in the coil inner-layer end blocks *a4_a5*. The quenches marked with circles started in the outer-layer midplane block *b2_b3* of coil #7 at 20 A/s. The dotted line in Fig. 9 shows the temperature dependence for the short sample current and the dashed line shows the expected quench current at different temperatures, but with the same ratio to the SSL as observed at 4.5 K. The plot suggests that there is a large critical current degradation in magnet coils.

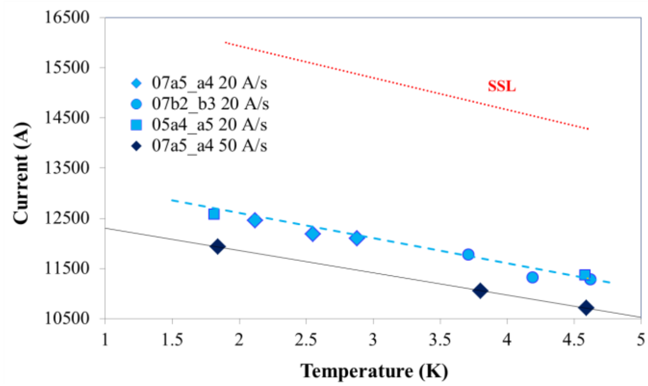

Fig. 9. Temperature dependence of quench current.

B. *Protection Heater Study*

Protection heater (PH) studies were focused on measurements of the quench delay time in the magnet operation current range, the radial quench propagation between the coil layers, and quench integral at 4.5 K and 1.9 K. Fig. 10 shows schematically the decay of magnet current and the coil voltage grows after the protection heater discharge at t=0.

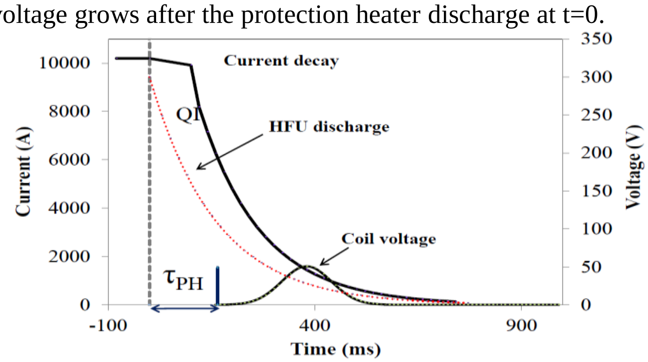

Fig. 10. Current decay and coil voltage development after HFU discharge.

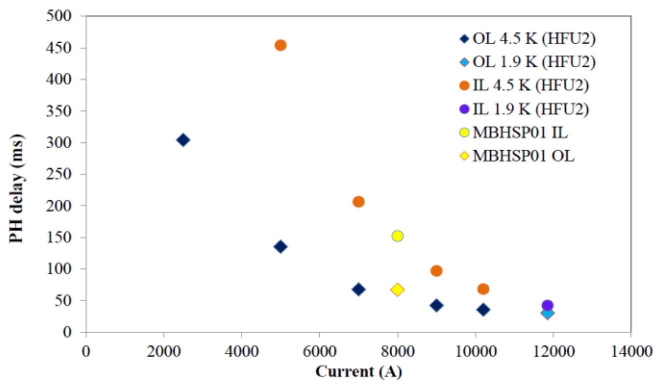

Fig. 11. Quench delay in the inner and outer layer vs. magnet current.

The minimum PH peak power density P_{AV} required to quench the magnet was measured at different currents. At the injection current level it was about 50-55 W/cm^2. Therefore, the heater studies in MBHSP02 were performed at P_{AV}=50-55 W/cm^2.

Simulations [12] and MBHSP01 heater studies [9] demonstrated that quench quite rapidly propagates in the radial direction from outer layer (OL) to inner layer (IL) coil blocks. Quench delay time was measured separately for OL and IL blocks both at 4.5 K and 1.9 K. To observe the quench propagation from the coil outer to the inner layer, the extraction dump was delayed by 1000 ms. Quench delay time was determined as the time between the heater ignition (t=0) and the voltage detection time in the coil (see Fig. 10). Figure 11 shows the quench delay time in the inner and outer layer vs. magnet current at P_{AV} =50 W/cm^2. The corresponding data measured at P_{AV}=25 W/cm^2 for similar heaters in MBHSP01 [9] are also shown, demonstrating excellent heater performance reproducibility. Short quench delay time observed at the high currents improves the dissipation of stored energy in magnet coil.

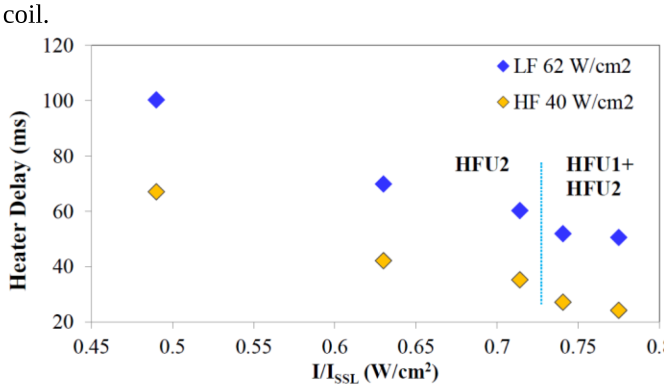

Fig. 12. Quench delay in LF and HF blocks vs. normalized magnet current.

Quench delay time was also measured for the low field (LF) and high field (HF) outer-layer blocks. The width of heater strips covering the LF and HF blocks is different and, thus, the peak power density is different in the LF and HF blocks: P_{LF} = 1.24·P_{AV}, P_{HF} = P_{AV}/1.24, where P_{AV} is average peak power density for both heaters in the LF and HF area. Measured quench delay time in the LF and HF blocks vs. magnet current is shown in Fig. 12. The difference in quench delay time for HF and LF blocks at the I_{nom} is only ~30 ms. This difference could be reduced or even completely eliminated by adjusting the heater power (e.g. heater width) in the HF and LF protection heaters.

Quench integral (QI) was determined by integrating $I^2(t)$ over the time from t=0 to t_{max}=1000 s (Fig. 10). Quench integral as a function of magnet current measured at 4.5 and 1.9 K for one and two heaters is shown in Fig. 13. The peak power density in PH was 50 W/cm^2 at 4.5 K and 55 W/cm^2 at 1.9 K. The quench integral at the nominal operation current of 11.85 kA reaches its maximum of 16 MIITs (for one protection heater) which corresponds to the maximum temperature T_{max} of the coil outer-layer under protection heaters less than 250 K (adiabatic conditions [12]). For two protection heaters operating simultaneously T_{max} under the heaters is less than 200 K.

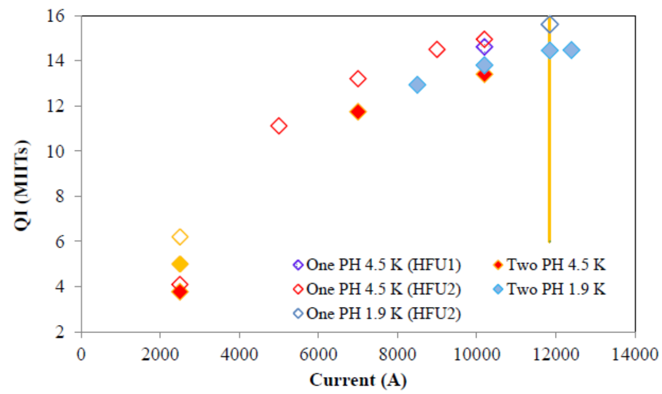

Fig. 13. Quench Integral vs. magnet current.

IV. Conclusion

The first of four 1 m long collared coils to be used in the twin-aperture Nb_3Sn dipole models has been built and tested at FNAL in a single-aperture configuration. The magnet reached 11.7 T at 1.9 K or 97.5% of its design field and demonstrated improved eddy current effect. The average RRR value was within 80-100, close to 80-120 range measured in MBHSP01 [3]. Yet, large quench current degradation, quite long magnet training and quenching at a current plateau were observed. The causes of that are being investigated.

Three new 1 m long coils with further improvements of the coil design and processing are being fabricated. The first coil will be tested in a dipole mirror configuration and the last two in a single-aperture configuration.

Experimental studies of magnet protection heaters were continued providing an important input to 11 T dipole quench protection system design and performance optimization.

Acknowledgment

The authors thank the staff of FNAL Technical Division for contributions to magnet design, fabrication and test.

References

[1] L. Bottura et al., “Advanced Accelerator Magnets for Upgrading the LHC”, *IEEE Trans. on Appl. Supercond.*, Vol. 22, Issue 3, 2012, p. 4002008.

[2] A.V. Zlobin et al., “Development of Nb_3Sn 11 T Single Aperture Demonstrator Dipole for LHC Upgrades”, *Proc. of PAC’2011*, NYC, 2011, p. 1460.

[3] A.V. Zlobin et al., “Development and test of a single-aperture 11T Nb_3Sn demonstrator dipole for LHC upgrades**”,** *IEEE Trans. on Appl. Supercond.*, Vol. 23, N 3, 2013, p. 4000904.
[4] M. Karppinen et al., “Design of 11 T Twin-Aperture Nb_3Sn Dipole Demonstrator Magnet for LHC Upgrades”, *IEEE Trans. on Appl. Supercond.*, Vol. 22, N 3, 2012, p. 4901504.
[5] G. Chlachidze et al., “Field Quality Study of a 1 m Long Single-Aperture 11 T Nb_3Sn Dipole Model for LHC Upgrades”, *this conference*.
[6] A.V. Zlobin et al., “Fabrication and Test of a 1-m Long Single-Aperture 11T Nb_3Sn Dipole for LHC Upgrades”, *Proc. of IPAC’2013,* Shanghai, China, May 2013, p. 3609.
[7] E. Barzi et al., “Superconducting Strand and Cable Development for the LHC Upgrades and Beyond,” *IEEE Trans. on Appl. Supercond.*, Vol. 23, Issue 3, 2013, p. 6001112.
[8] N. Andreev *et al.*, “Volume expansion of Nb_3Sn strands and cables during heat treatment”, *Adv. in Cryo. Engineer.*, vol. 48, AIP, 2002, p. 941.
[9] G. Chlachidze et al., “Quench protection study of a single-aperture 11T Nb_3Sn demonstrator dipole for LHC upgrades”, *IEEE Trans. on Appl. Supercond.*, Vol. 23, Issue 3, June 2013 Page 4001205.
[10] I. Novitski et al., “Study of Mechanical Models of a Single-Aperture 11 T Nb_3Sn Dipole”, *IEEE Trans. on Appl. Supercond*., Vol. 23, Issue 3, June 2013 Page 4001804.
[11] M.J. Lamm et al., “A New Facility to Test Superconducting Accelerator Magnets”, *Proc. of PAC1997*, Vancouver, 1997, p. 3395.
[12] A.V. Zlobin, I. Novitski, R. Yamada, “Quench Protection Analysis of a Single-Aperture 11T Nb_3Sn Demonstrator Dipole for LHC Upgrades”, *Proc. of IPAC’2012*, New Orleans, Louisiana, USA, p.3599.